Axion Detection with Resonant Cavities

Kelsey Oliver-Mallory

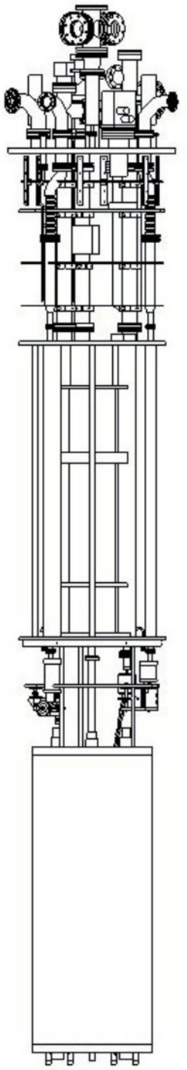

Content

- Axions (why resonant cavities are an effective way to detect them)
- Resonant Cavities (how they work)
- ADMX (limits that cut into region of plausible axion theories)

Axions

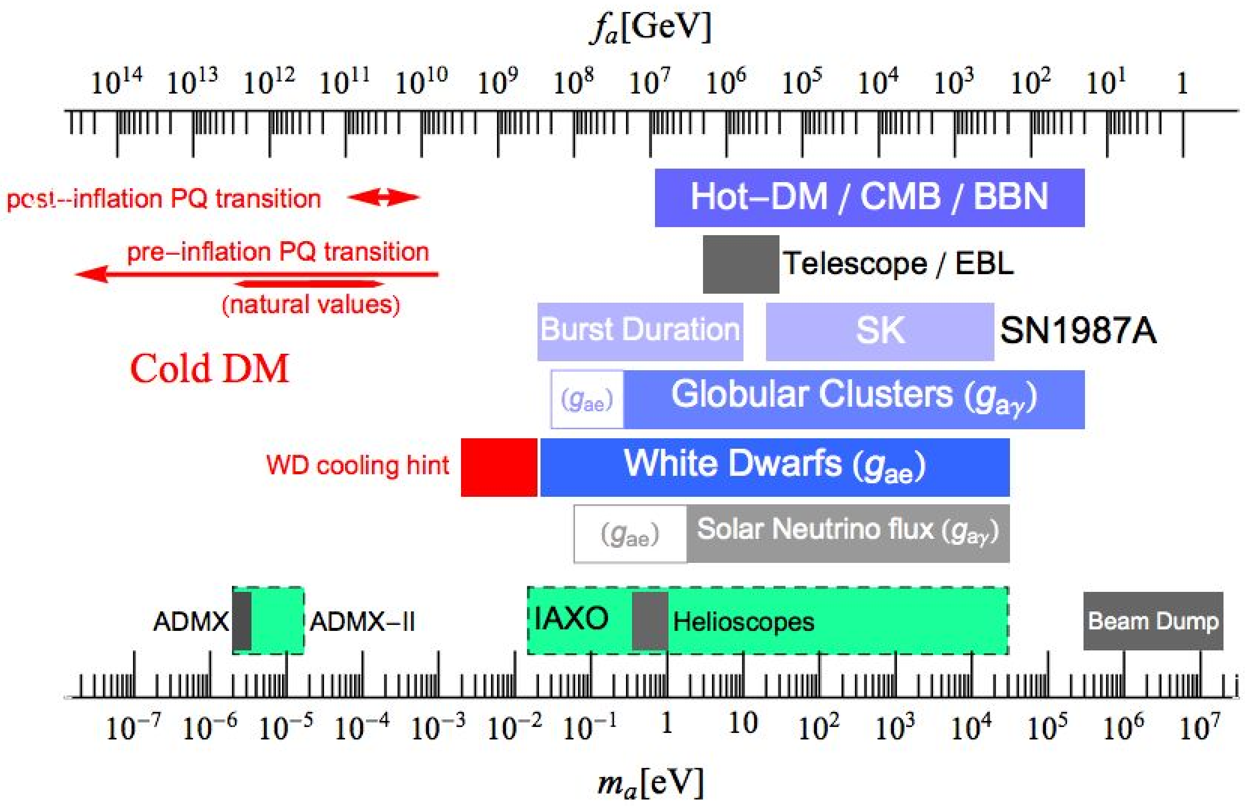

- pseudoscalar dark matter candidate
- probably light
- probably cold

Peccei-Quinn Theory

$$\mathcal{L} = \left(\bar{\Theta} - \frac{\phi_A}{f_A}\right) \frac{\alpha_s}{8\pi} G^{\mu\nu a} \tilde{G}^a_{\mu\nu}$$

- Strong force only breaks charge parity
- Strong CP problem
- Breaks hidden global U[1] symmetry
- pseudo-Nambu-Goldstone boson
- meets dark matter requirements: cold, non-baryonic, weak coupling to normal matter
- Forms a Bose_Einstein condensate

Mass

$$m_A = \frac{z^{1/2}}{1+z}\frac{f_\pi m_\pi}{f_A} = \frac{0.60\ \text{meV}}{f_A/10^{10}\,\text{GeV}}$$

$$f_a \gtrsim 10^9\ \text{GeV} \qquad f_a \gtrsim 10^{12}\ \text{GeV}$$

$$m_a = 1\ \mu\text{eV},\ \tau_{1/2} \approx 10^{54}\ \text{s}$$

- fA is the decay constant
- constrained cosmic observation and particle physics experiments
- SN1987A: lower bound f_A
- cosmic energy density: upper bound on f_A
- Axion mass in range: ueV-meV
- Lifetime much greater than age of universe

Coupling to photon (KSVZ and DFSZ models)

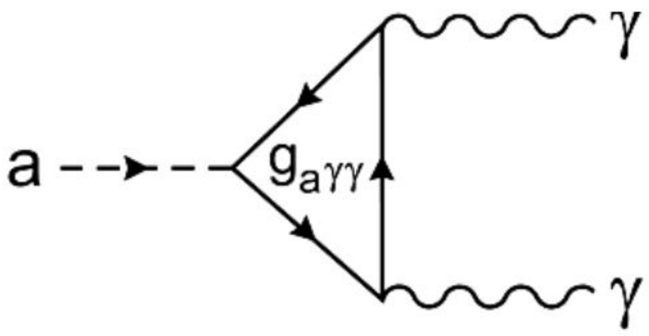

$$\mathcal{L}_{a\gamma\gamma} = g_{a\gamma\gamma} a \boldsymbol{E} \cdot \boldsymbol{B}$$

$$g_{a\gamma\gamma} = \frac{\alpha g_\gamma}{2\pi f_a}$$

$$g_{a\gamma\gamma}^{\mathrm{KSVZ}} \approx 0.38 \frac{m_a}{\mathrm{GeV}^2}$$

$$g_{a\gamma\gamma}^{\mathrm{DFSZ}} \approx 0.14 \frac{m_a}{\mathrm{GeV}^2}$$

- ***α*** is the fine structure constant
- g_γ is a model dependent coupling constant

Inverse Primakoff Effect

- Use B_0 as a virtual photon
- Increase decay rate by increasing external magnetic field

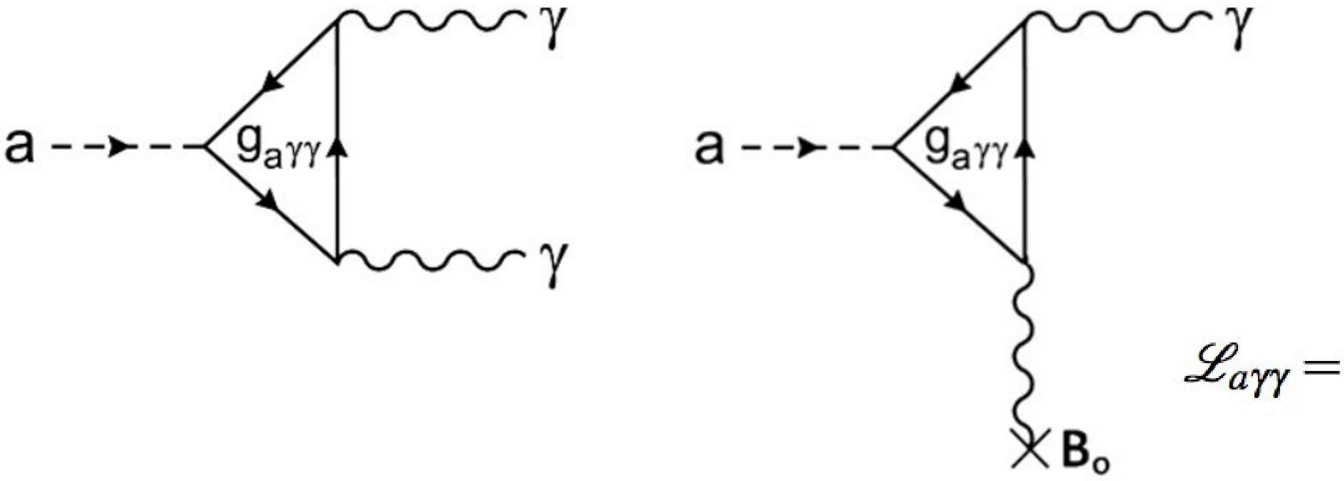

$$\mathcal{L}_{a\gamma\gamma} = g_{a\gamma\gamma} a \boldsymbol{E} \cdot \boldsymbol{B}$$

FIGURE 1. Feynman diagram of axion decay into photons. Left) Conversion in vacuum. Right) Inverse Primakoff effect in a static magnetic field ($\mathbf{B_o}$).

Resonant Cavities for Axion Detection

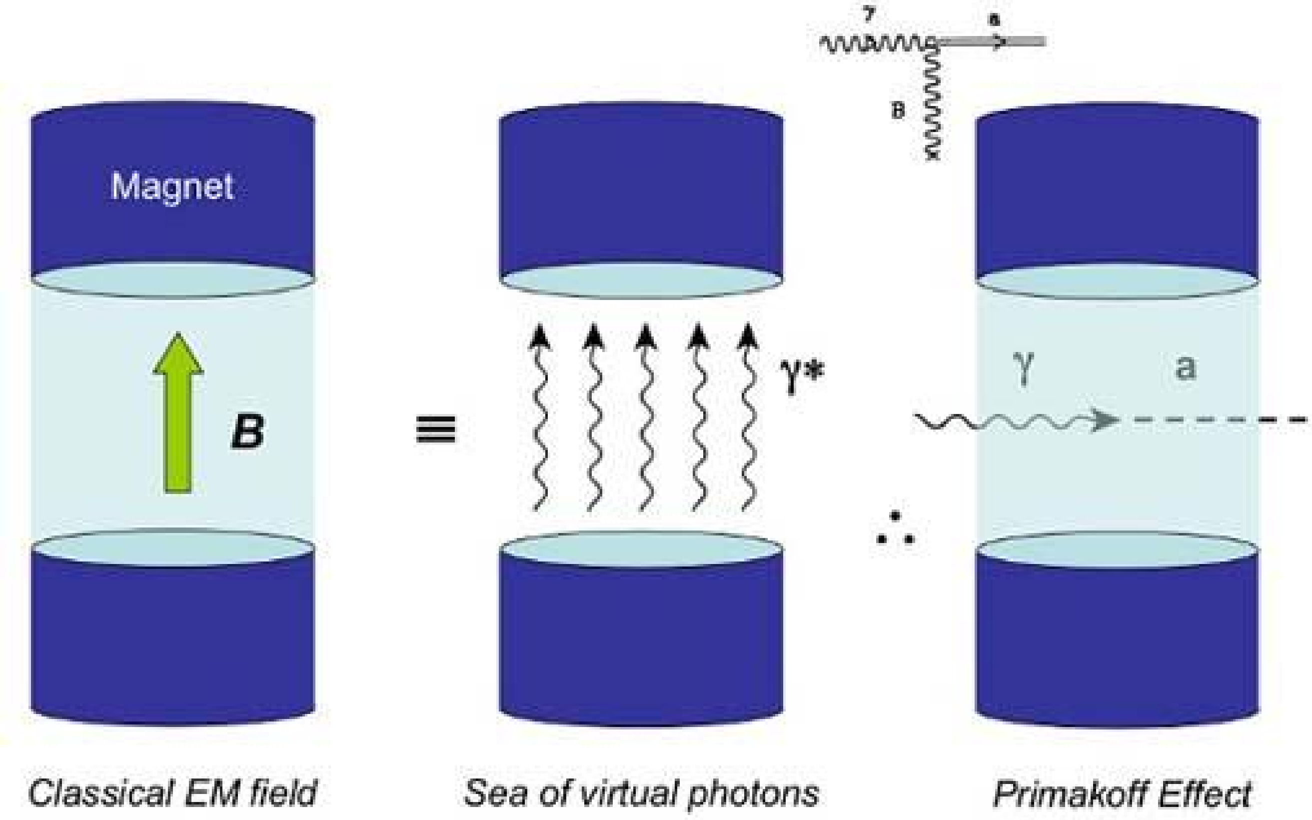

- Use a long cylindrical resonant cavity
- Apply uniform magnetic field throughout cavity
- Can detect photons at resonant frequencies

Resonant Cavities for Axion Detection

- Maxwell's equations and boundary conditions result in standing waves
- Only certain resonant modes allowed
- Energy of axion must align with frequency of resonant mode
- Usually looking for TM010 mode.

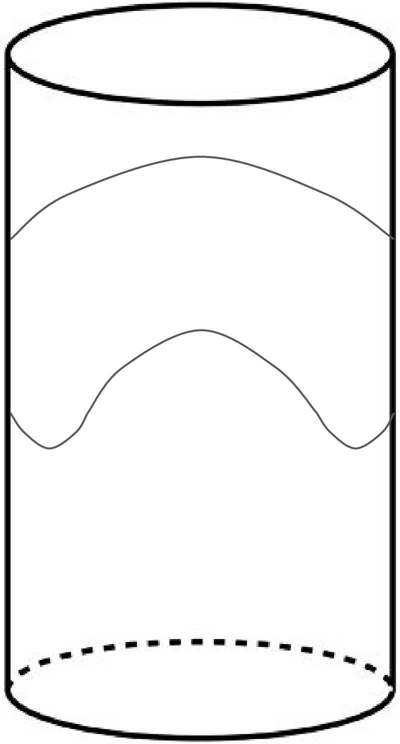

TM_{010} mode in a pill-box cavity

$$E_r = 0,$$
$$E_z = E_0 J_0 (k_r r) \cos(\omega t),$$
$$H_\varphi = -\frac{E_0}{Z_0} J_1 (k_r r) \sin(\omega t)$$

$$f \approx \frac{m_a c^2}{h}$$

Resonant Cavities for Axion Detection

- Want tunable resonant cavities
- Position of rods changes the resonant frequency

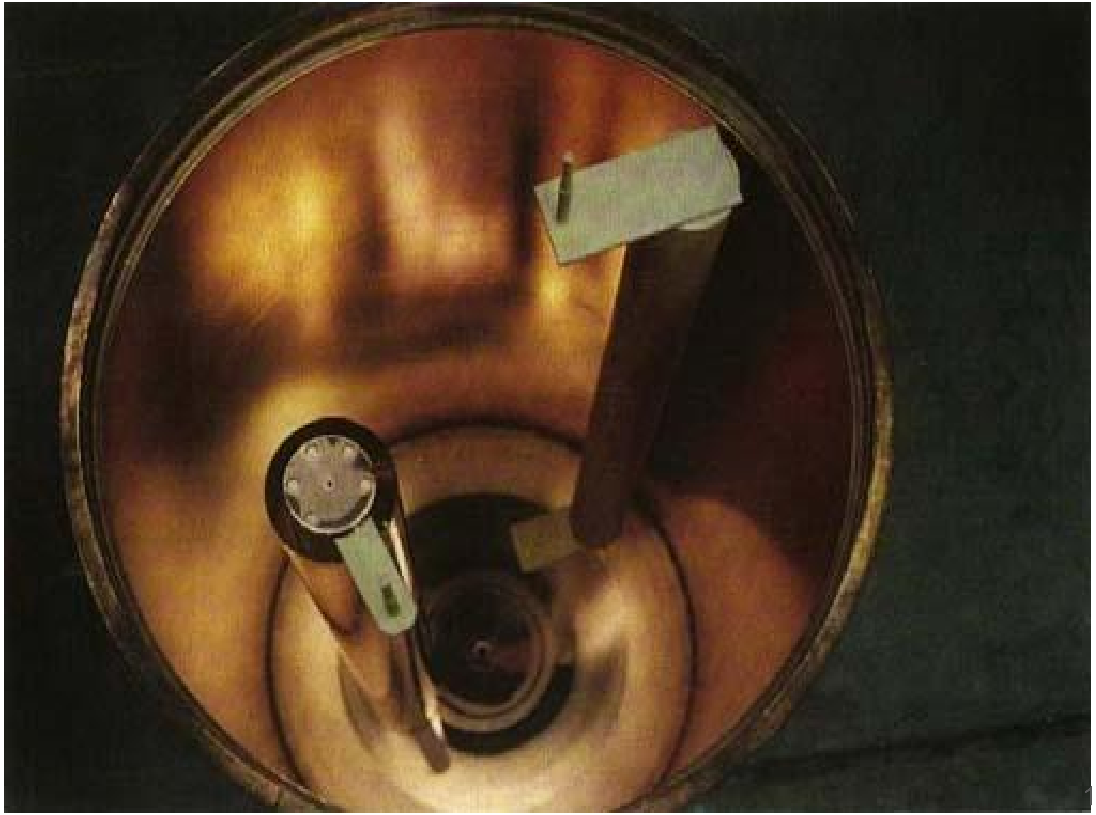

Tuning Resonant Modes

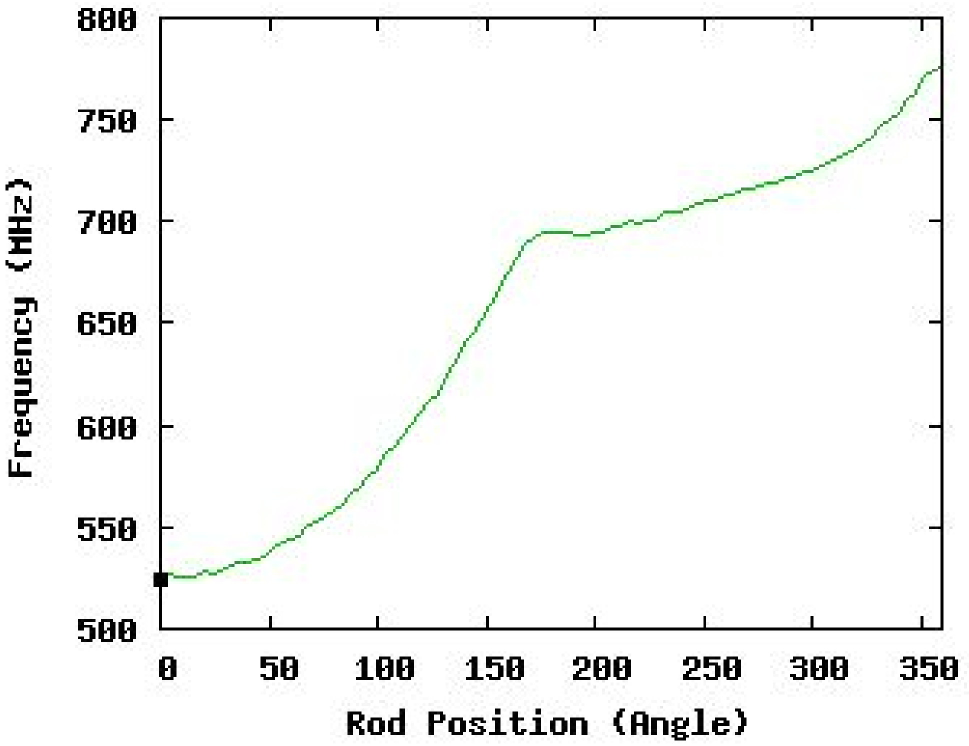

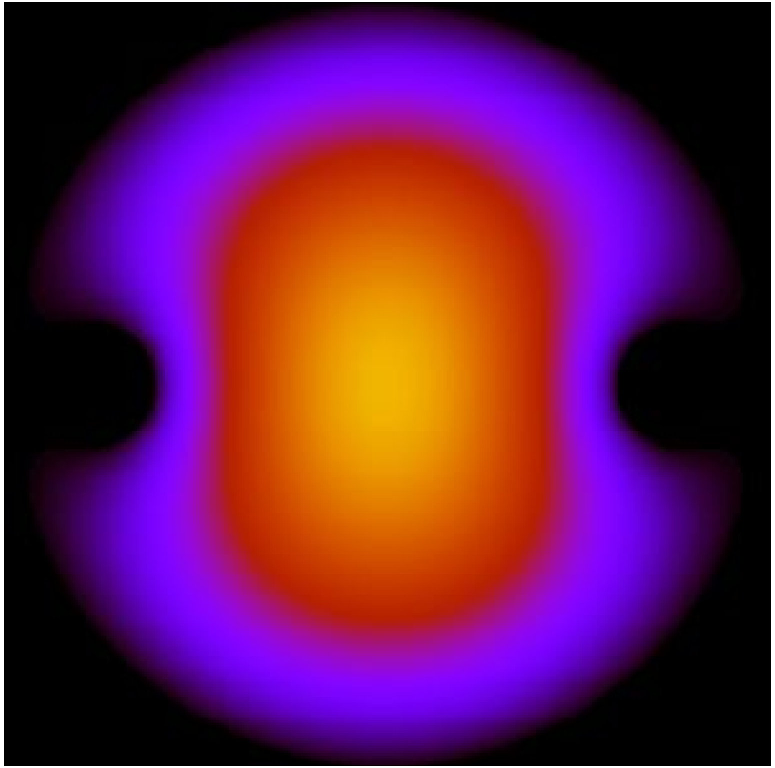

- Magnitude electric field

Tuning Resonant Modes

- Power produced in cavity from axion
- ρ_a: local energy density of axion field
- V: volume of the cavity
- Q_L: loaded quality factor
- Cmnp: coupling form factor of the axion to a specific mode

$$P_{mnp} = g_{a\gamma\gamma}^2 \frac{\rho_a}{m_a} B_o^2 V C_{mnp} Q_L = 10^{-22} \text{ W}$$

$$\int d^3x \boldsymbol{B_o} \cdot \boldsymbol{E_{mnp}}(x), \quad g_{a\gamma\gamma} = \frac{\alpha g_\gamma}{2\pi f_a}$$

$$C_{mnp} = \frac{\left| \int_V d^3x \boldsymbol{B_o} \cdot \boldsymbol{E_{mnp}}(x) \right|}{B_o^2 V \int_V d^3x \, \varepsilon(x) |\boldsymbol{E_{mnp}}(x)|^2}$$

Comparison Resonant Cavity Experiments

- Projected limits for ADMX move into band of viable theories.

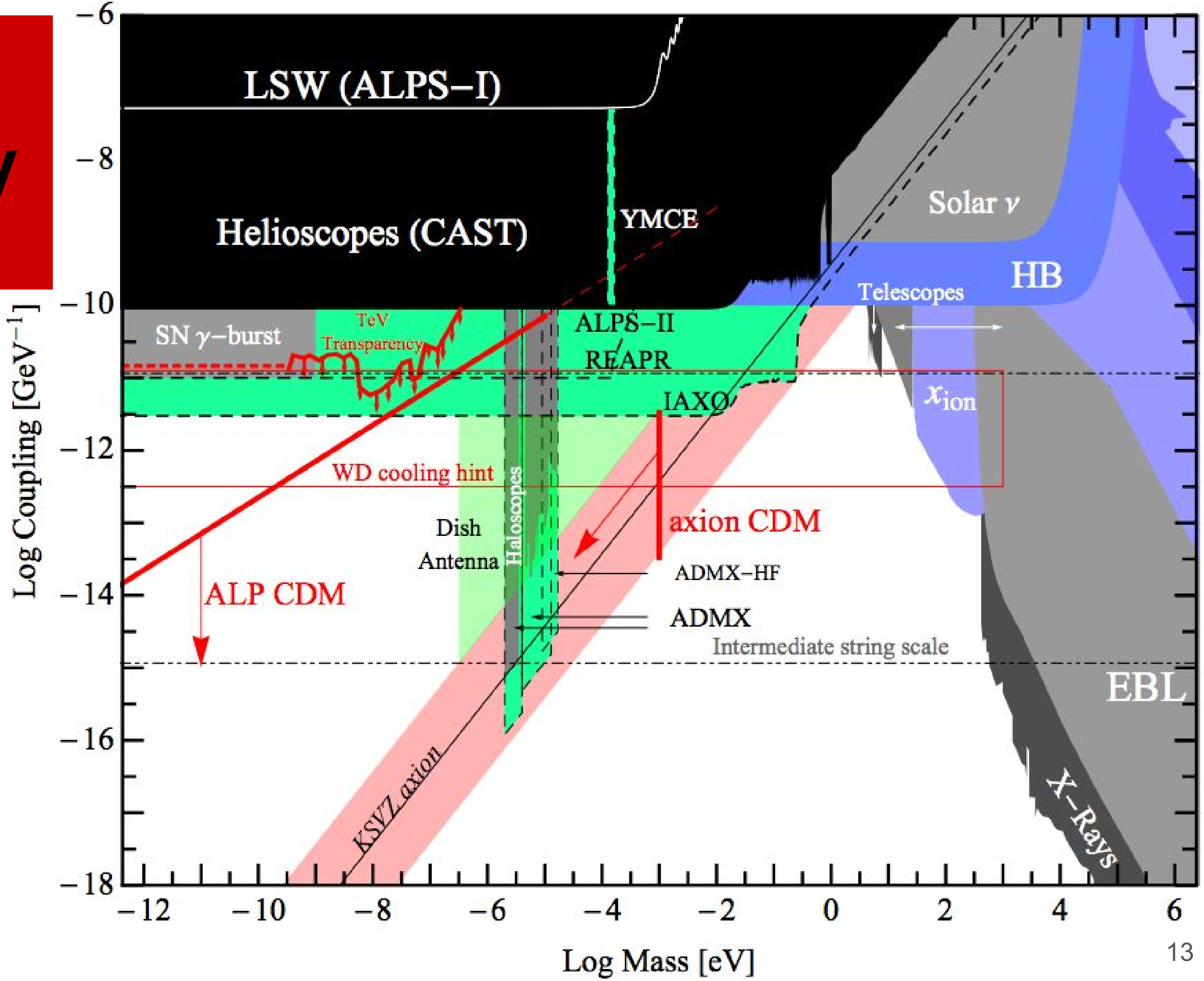

ADMX Detector

- Superconducting solenoid
- 7.6 Tesla magnetic field
- Cylindrical resonant cavity: r=21cm and z= 100cm
- Black body and axion photons picked up by antenna at top of cavity
- Cryogenically cooled

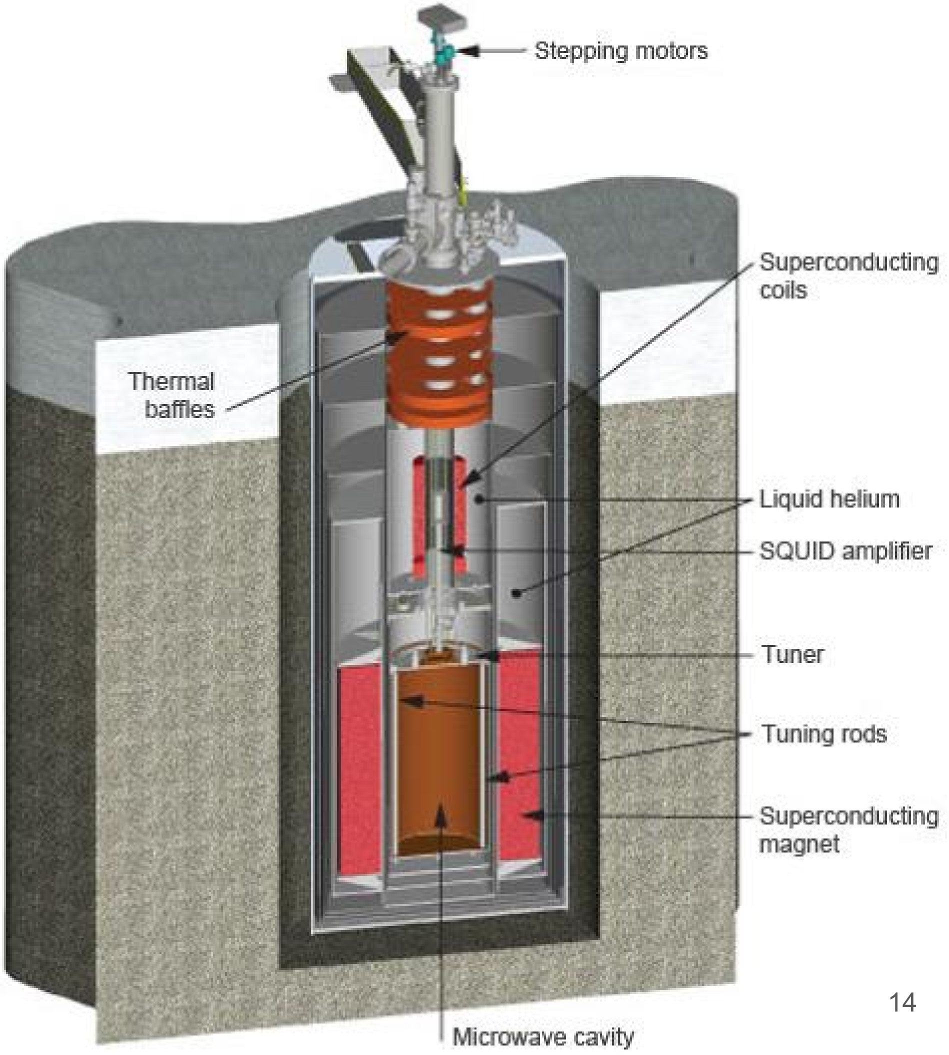

ADMX Detector

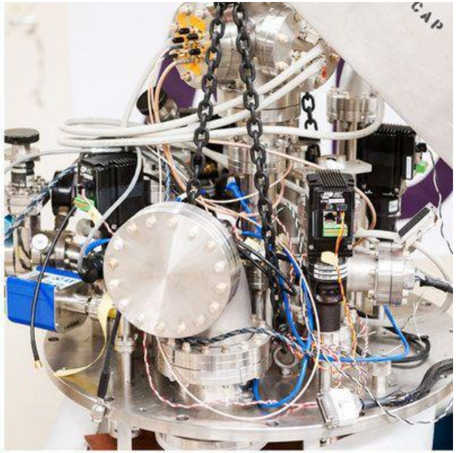

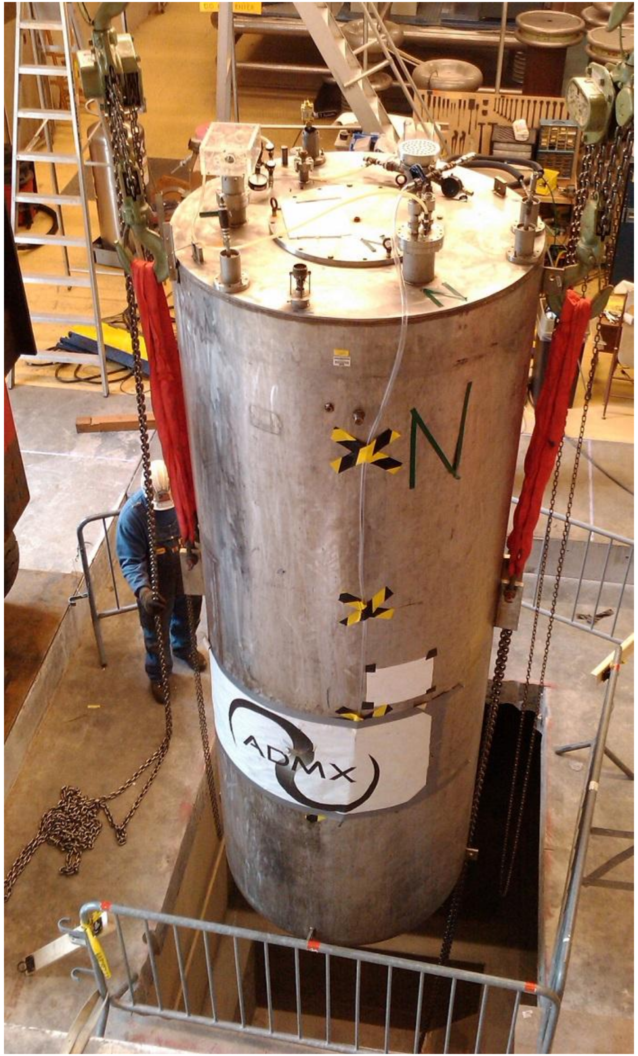

Receiver and Electronics

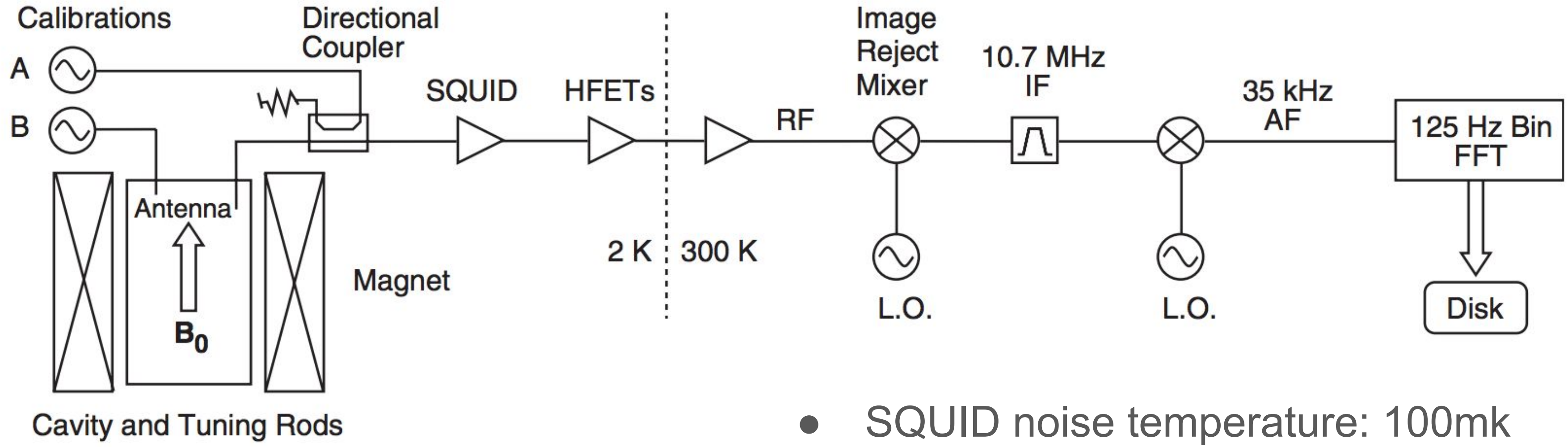

- HFET noise temperature: 2K
- KSVZ axions: 1.9-3.3 ueV

- SQUID noise temperature: 100mk at 500MHz and 200mK
- KSVZ axions: 3.3-3.53 ueV
- Newest version: cooling with 3He/4He dilution refrigerator

SQUIDs

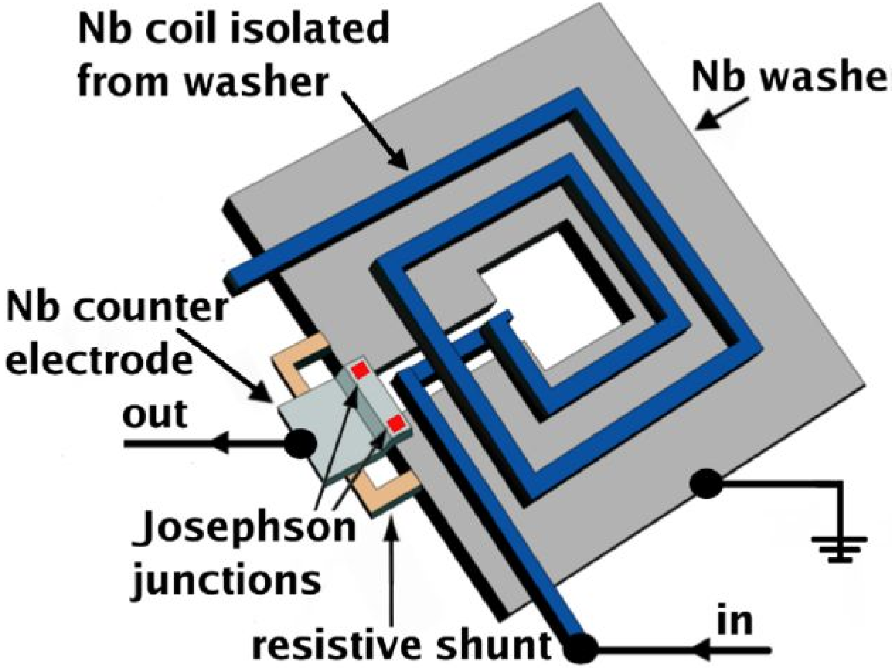

FIG. 2 (color online). Schematic of a microstrip SQUID amplifier.

Signal

- Warm power spectrum with cavity resonance
- Monte Carlo with axions

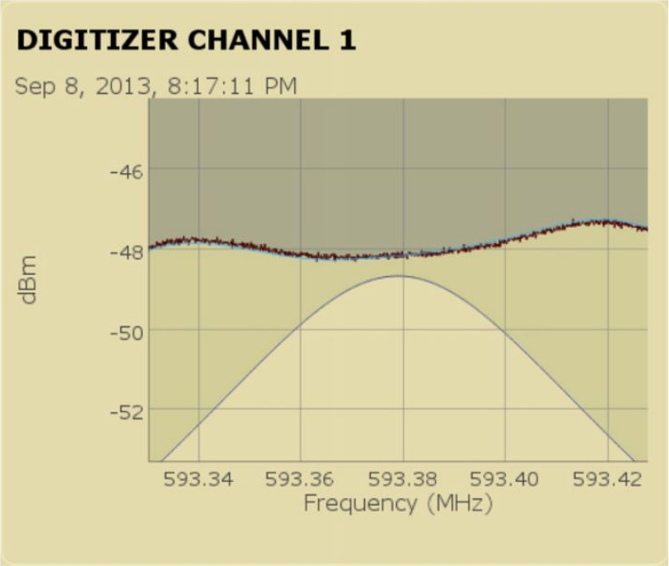

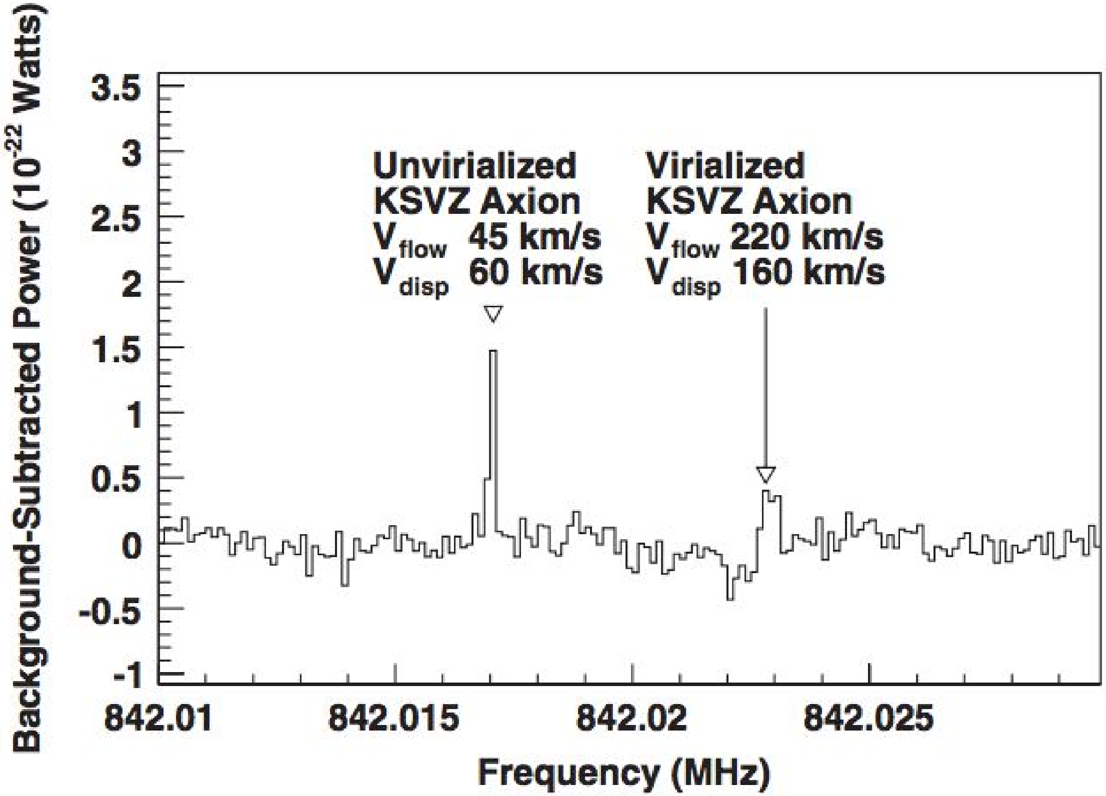

FIG. 4. Dark-matter axion signals simulated with Monte Carlo calculations and imposed on real data for two dark-matter axion distribution models. Example masses chosen to appear at 842.017 MHz and 842.023 MHz.

ADMX Sensitivity

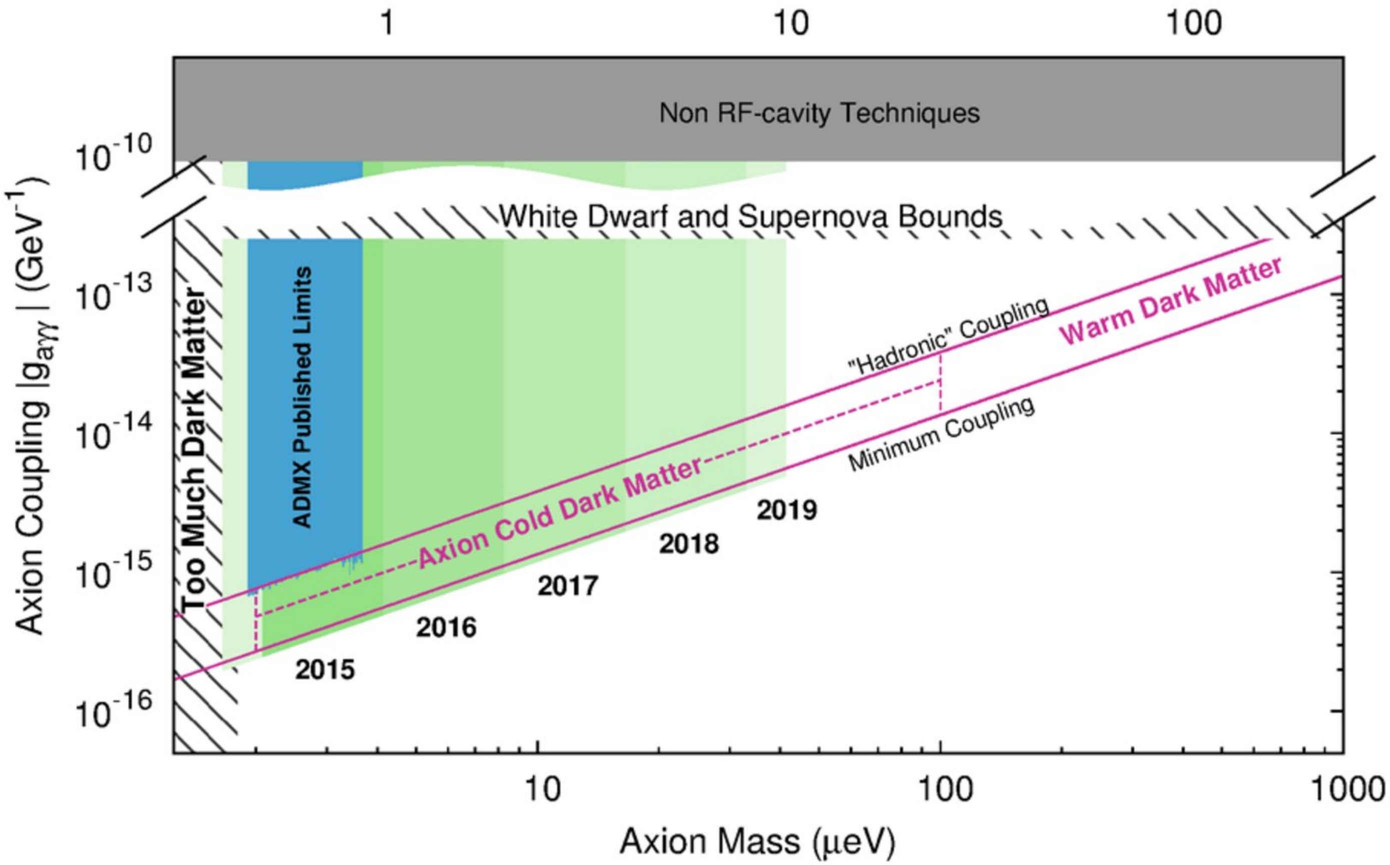

End of Presentation

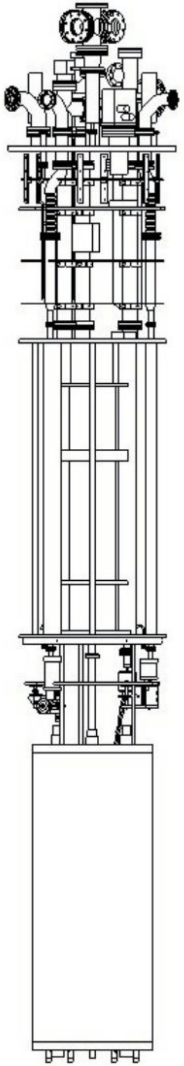

SQUIDs

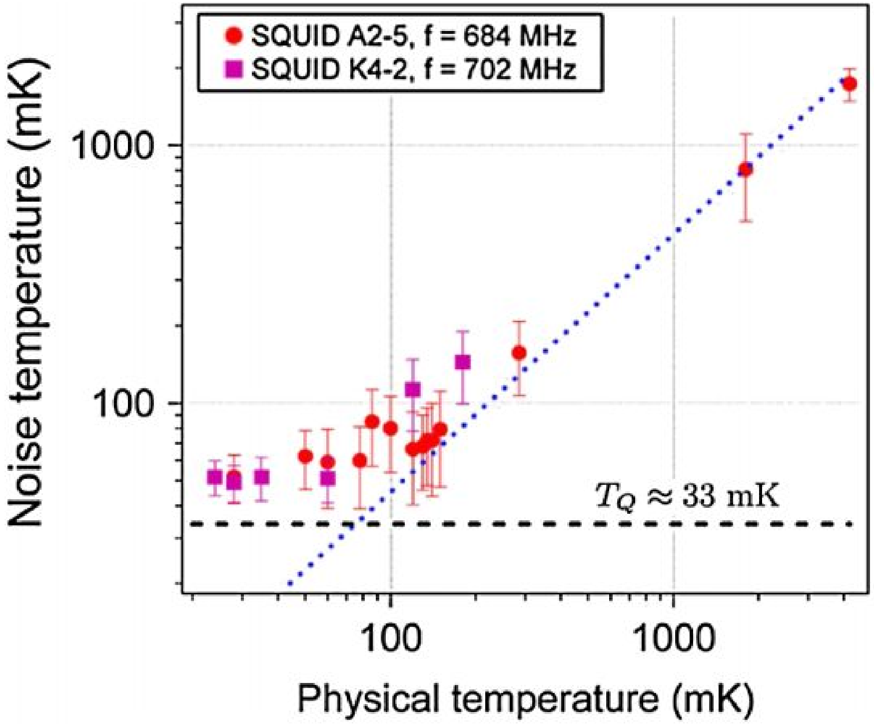

FIG. 3 (color online). Noise temperature of two representative SQUID amplifiers (with resonant frequency f) as a function of physical temperature. Dashed line indicates T_Q, the quantum noise temperature at ≈700 MHz. Dotted line has a unity slope, indicating that $T_A \propto T$ in the classical regime.